Journal of Alloys and Compounds 509 (2011) 2420–2424

Contents lists available at ScienceDirect

Journal of Alloys and Compounds

journal homepage: www.elsevier.com/locate/jallcom

Effects of the co-addition of $LiSbO_3$–$LiTaO_3$ on the densification of $(Na_{1/2}K_{1/2})NbO_3$ lead free ceramics by atmosphere sintering

Na Jiang, Bijun Fang*, Jian Wu, Qingbo Du

School of Materials Science and Engineering, Changzhou University, Changzhou, Jiangsu 213164, People's Republic China

ARTICLE INFO

Article history:
Received 27 July 2010
Received in revised form 13 October 2010
Accepted 7 November 2010
Available online 13 November 2010

Keywords:
$(Na_{1/2}K_{1/2})NbO_3$ lead-free ceramics
Solid-state reaction
Perovskite structure
Electrical properties
Doping

ABSTRACT

Pure phase perovskite $0.94(Na_{1/2}K_{1/2})NbO_3$–$0.03LiSbO_3$–$0.03LiTaO_3$ (0.94NKN–0.03LS–0.03LT) lead-free piezoelectric ceramics were prepared by the conventional solid-state reaction method. Due to the co-addition of $LiSbO_3$–$LiTaO_3$, the 0.94NKN–0.03LS–0.03LT ceramics prepared by atmosphere sintering at 1040 °C exhibit high relative density, being 94.73%, and rather homogenous microstructure. X-ray diffraction (XRD) measurement confirmed that the sintered ceramics exhibit pure tetragonal perovskite structure. The 0.94NKN–0.03LS–0.03LT ceramics exhibit excellent integral electrical properties, in which the value of piezoelectric constant d_{33} is 228 pC/N, the electromechanical coupling factors K_p and K_t are 0.220 and 0.230, respectively, the mechanical quality factor Q_m is 32.19, and the remnant polarization P_r is 23.06 μC/cm^2. Such excellent electrical properties are considered as correlating with the high relative density of the synthesized ceramics induced by the co-doping of $LiSbO_3$–$LiTaO_3$.

1. Introduction

Over the past half century, most piezoelectric ceramic devices such as filters, resonators, actuators, sensors, and so on, were fabricated by using lead-based piezoelectric ceramics such as $Pb(Zr_xTi_{1-x})O_3$ (PZT) due to their superior piezoelectric properties [1–3]. However, due to the volatile and toxic nature of PbO, environmental problems were caused during the processing and disposition processes of the lead-based ceramics. For these reasons, much work has recently been focused on lead-free ferroelectrics [4,5]. Among which, $(Na_{0.5}K_{0.5})NbO_3$ (NKN) has been considered as a good candidate for the lead-based piezoelectric ceramics because of its large piezoelectricity and ferroelectricity. The hot pressed NKN ceramics have been reported to possess a high Curie temperature [6–9], which exhibit about 99% of the theoretical density. However, the pure NKN ceramics are difficult to densify fully by ordinary sintering method because the phase stability of pure NKN is 1140 °C, which makes it impossible to prepare the pure NKN ceramics with high density by atmosphere sintering [10]. Furthermore, the volatility of the potassium oxide makes the stoichiometry difficult to control, and the formation of extra phases leads to a quick disintegration of the final samples once exposed to humidity (deliquescence) [3]. Therefore, various techniques, such as hot pressing [8], cold-isostatic pressing [10], and spark plasma sintering [11], have been utilized to improve the electrical properties of the pure NKN ceramics. Since these techniques were unsuitable for use in industrial production, many studies have been conducted in order to prepare the NKN-based ceramics by the conventional solid-state sintering method and without the cold-isostatic pressing (CIP) process.

From the industrial point of view, atmospheric sintering is beneficial for mass production [12]. The incorporation of $LiTaO_3$ into the perovskite structure NKN improves piezoelectric property [7]. Recently, Guo et al. reported that it was able to obtain excellent piezoelectric and electromechanical response with the composition near the morphotropic phase boundary (MPB) $0.95Na_{0.5}K_{0.5}NbO_3$–$0.05LiTaO_3$ (0.95NKN–0.05LT) through the conventional sintering method [13]. However, the sintering temperature of this system was too high (1100 °C) to inhibit the volatilization of K_2O [7]. It is generally accepted that the addition of Sb_2O_3 can enhance stability and compactness of the NKN ceramics, which will also offer a high electromechanical coupling factor [14].

In this paper, the NKN-based lead-free ceramics were densified by the co-addition of $LiSbO_3$–$LiTaO_3$ (LS–LT) through the conventional ceramic processing by atmosphere sintering. Previous works revealed that electrical properties of the NKN ceramics can be improved by the doping of LS or LT up to the content of 5 mol%, respectively [13–15]. Therefore, the concentration of the co-addition of LS–LT was up to 10 mol%, and the mole ratio of the both dopants was tailored. Preliminary experiments proved that $0.94(Na_{1/2}K_{1/2})NbO_3$–$0.03LiSbO_3$–$0.03LiTaO_3$ (0.94NKN–0.03LS–0.03LT) exhibits pure tetragonal perovskite structure and excellent integral electrical properties. In this work,

* Corresponding author. Tel.: +86 519 86330095; fax: +86 519 86330095.
E-mail addresses: fangbj@sohu.com, fangbj@cczu.edu.cn (B. Fang).

0925-8388/$ – see front matter © 2010 Elsevier B.V. All rights reserved.
doi:10.1016/j.jallcom.2010.11.033

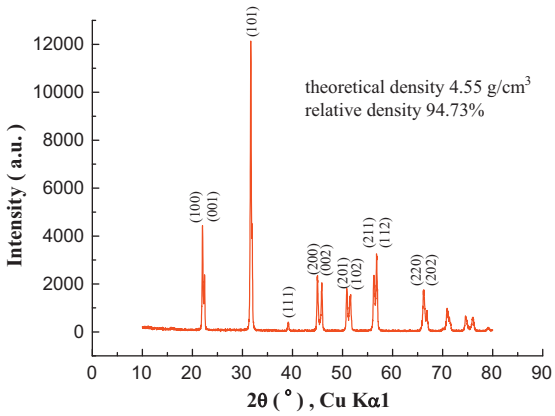

Fig. 1. XRD pattern of the 0.94NKN–0.03LS–0.03LT ceramics sintered at 1040 °C for 2 h.

the synthesis of the 0.94NKN–0.03LS–0.03LT lead-free piezoelectric ceramics by the conventional solid-state reaction method was reported, and the influences of the dopants on the phase structure, microstructure morphology and electrical properties were studied systematically.

2. Experimental procedure

The 0.94NKN–0.03LS–0.03LT ceramics were prepared by the conventional solid-state reaction method sintered at air pressure. Analytical-purity carbonates and oxides, Na_2CO_3 (99.8%), K_2CO_3 (99.0%), Nb_2O_5 (99.5%), Li_2CO_3 (98.0%), Sb_2O_3 (99.0%) and Ta_2O_5 (99.99%) were used as raw materials. In order to obtain stoichiometric composition, the raw materials were dried separately before weighing. Well-mixed stoichiometric raw materials were calcined at 850 °C for 9 h. The calcined powders were dry-pressed into pellets with 12 mm in diameter with the addition of about 1 wt% polyvinyl alcohol (PVA, the concentration of the PVA water solution is 8 wt%) binder and sintered in air at 1040 °C for 2 h. Such sintering conditions were adopted since preliminary experiments proved that the 0.94NKN–0.03LS–0.03LT ceramics sintered at 1040 °C exhibit high relative density and excellent electrical properties. The pellets were buried under an equiweight mixture of the raw materials with the same composition in a covered crucible to minimize the evaporation of the alkali metal cations during sintering.

The sintered ceramics were ground and polished to obtain flat and parallel surfaces. Crystal structure of the sintered ceramics was measured by X-ray diffraction measurement (XRD, Rigaku D/max-2500/PC X-ray diffractionmeter) using the well-polished pellets. Microstructure morphology of the sintered ceramics was observed by scanning electron microscopy (SEM, JSM6360LA) using free surfaces of the specimens after thermal etching at 850 °C for 60 min. For electrical properties characterization, silver paste was fired on both surfaces of the well-polished ceramics as electrodes. Dielectric property was measured using a computer-interfaced TH2818 automated analyzer combining with a programmable furnace from 20 to 450 °C. For the measurements of piezoelectric and electromechanical properties, the ceramics were poled under an electrical field of 3.67 kV/mm at 100 °C for 15 min in silicon oil and then slowly cooled down to room temperature with maintaining 1 kV/mm electric field. Piezoelectric property was measured by a ZJ-3AN Berlincourt-type quasistatic d_{33} meter. The electromechanical coupling coefficient and the mechanical quality factor Q_m were determined by resonance–antiresonance method using a TH2826 High Frequency LCR Meter. Detailed electrical properties measurement procedures were described elsewhere [15].

3. Results and discussion

3.1. Phase structure and microstructure morphology

Fig. 1 shows XRD pattern of the 0.94NKN–0.03LS–0.03LT ceramics sintered at the optimized conditions, where the influence of the co-addition of LS–LT on the crystal structure of NKN can be investigated. The diffraction peaks of the 0.94NKN–0.03LS–0.03LT ceramics are indexed based on the JCPDS data of tetragonal $KNbO_3$ (JCPDS 71-0948). Pure perovskite structure can be obtained for the 0.94NKN–0.03LS–0.03LT ceramics prepared by this method. Due to the solid solution of LS–LT into the NKN-based ceramics, the {1 0 0}, {2 0 0}, {2 1 0}, {2 2 0} diffraction reflections exhibit apparent doubly splitting, and the other diffraction reflections exhibit broadened single peaks, indicating that 0.94NKN–0.03LS–0.03LT exists in tetragonal perovskite structure with some distortion. As a comparison, for the pure NKN ceramics prepared by the same method, {1 0 0}, {1 1 0} diffraction reflections exhibit apparent doubly splitting, and {2 0 0}, {2 1 0} diffraction reflections exhibit triply splitting, indicating that tetragonal phase and orthorhombic phase coexist in NKN. The room-temperature crystal structure changes from orthorhombic perovskite structure of NKN to tetragonal one of 0.94NKN–0.03LS–0.03LT, which is considered as correlating with the slight difference of ionic radius between Nb^{5+}, Sb^{5+} and Ta^{5+} (ionic radii of Nb^{5+}, Sb^{5+} and Ta^{5+} are 0.64 Å, 0.6 Å and 0.64 Å, respectively), the small ionic radius of Li^+ as compared to that of Na^+ and K^+ (ionic radii of Na^+, K^+ and Li^+ are 1.02 Å, 1.38 Å and 0.76 Å, respectively), and the distortion of the perovskite cell lattice [16]. The sintered 0.94NKN–0.03LS–0.03LT ceramics exhibit large relative density, which reaches 94.73% of the theoretical density, confirming that such sintering conditions are optimum.

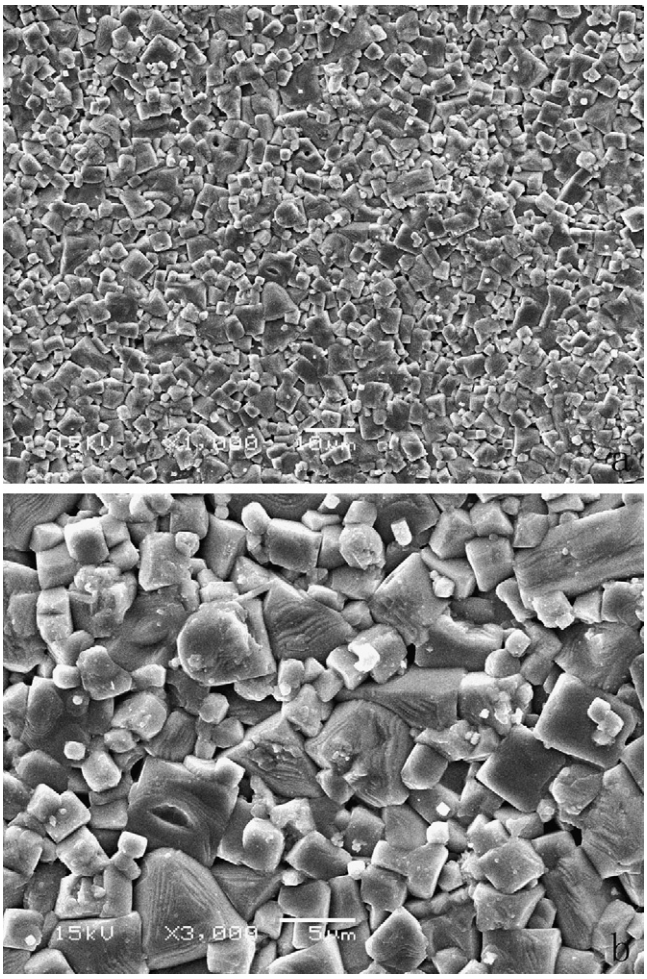

Fig. 2. SEM images of the 0.94NKN–0.03LS–0.03LT ceramics sintered at 1040 °C for 2 h: (a) 1000× and (b) 3000×.

Microstructure morphology of the 0.94NKN–0.03LS–0.03LT ceramics synthesized at the optimized conditions is shown in Fig. 2. As compared to the polyhedral micro-morphology of the pure NKN ceramics, indicating that solid-state sintering mechanism takes major effect in the densification of the ceramics, the 0.94NKN–0.03LS–0.03LT ceramics exhibit rather homogeneous microstructure, where the distribution of grains becomes more uniform and almost no pores are observed. Such results

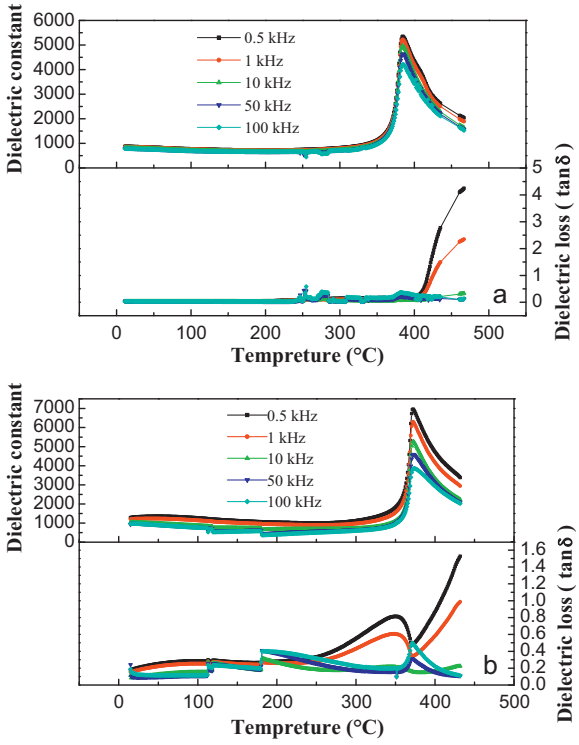

Fig. 3. Temperature dependence of dielectric constant and loss tangent of the 0.94NKN–0.03LS–0.03LT ceramics measured at several frequencies upon heating: (a) unpoled and (b) poled.

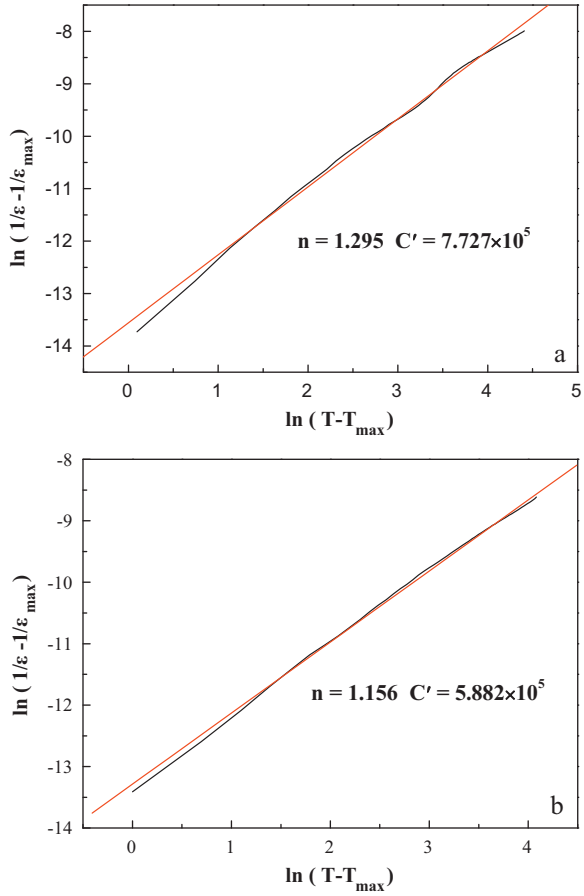

Fig. 4. Dielectric response character of 0.94NKN–0.03LS–0.03LT measured at 1 kHz upon heating. The fitting parameters obtained by the linear regression analysis are shown in the plot: (a) unpoled and (b) poled.

correspond well with the density data measured. The sintered 0.94NKN–0.03LS–0.03LT ceramics exhibit large bulk density, being 4.31 g/cm^3, which reaches 94.73% of the theoretical density. The density of the NKN-based ceramics correlates with the evaporation of alkali metal oxides, the elimination of pores, the growth of grain size and the densification of ceramics during sintering. Although most grains exhibit polyhedral micro-morphology, many grains exhibit round microstructure and the grain boundaries become obscure indicating that the liquid-phase sintering mechanism is inevitably taking partial effect in the densification of the 0.94NKN–0.03LS–0.03LT ceramics. Due to the low melting points of Li_2CO_3 (618 °C) and Sb_2O_3 (656 °C) [9], liquid phase forms at a relatively low temperature [16], which improves the sintering ability of the NKN-based ceramics. Therefore, the co-addition of LS–LT can prepare the NKN-based ceramics with high density by atmosphere sintering. In the larger magnification SEM image, grain morphology, grain size and grain boundaries can be seen clearly.

3.2. Dielectric property

Dielectric property of the 0.94NKN–0.03LS–0.03LT ceramics is shown in Fig. 3. For the pure NKN ceramics prepared by the same solid-state reaction method, three relatively distinct dielectric response peaks appear in the dielectric–temperature plots. The dielectric peak appearing at 406 °C is characteristic of ferroelectrics and is considered as relating to the phase transitions from tetragonal ferroelectric phase to cubic paraelectric phase transition. Such ferroelectric phase transition is induced by the coupling of the distortion of the octahedras in the perovskite structure and the large spontaneous polarization. Additional two small dielectric response peaks appear at 200 °C and 360 °C, which can be attributed to the phase transition from orthogonal ferroelectric phase to tetragonal ferroelectric phase and maybe correlate with the disorder distribution of cations in the A-site of the perovskite structure and/or the formation of micro-domain clusters, respectively [15]. Due to the co-addition of LS–LT, before poling, only unique dielectric peak appears of the 0.94NKN–0.03LS–0.03LT ceramics. As compared to the pure NKN ceramics, the temperature of dielectric maximum T_m decreases to a lower temperature around 384.7 °C, the dielectric response peaks sharpen, and the dielectric frequency dispersion weakens to some extent.

Dielectric property is influenced by the poling process. As compared to the unpoled 0.94NKN–0.03LS–0.03LT ceramics, T_m decreases and the value of dielectric maximum ε_m increases accompanied by the enhancement of frequency dispersion especially around T_m, where T_m decreases from 384.7 °C to 372.5 °C and ε_m increases from 5351 to 6961. The variation of the values of T_m and ε_m can be attributed to the poling process, where the stabilization of ferroelectric domains, the growth, orientation and movement of domain walls are influenced [17,18]. Dielectric loss increases slightly accompanied by a slight decrease of the temperature of the loss tangent maximum of the poled 0.94NKN–0.03LS–0.03LT ceramics as compared to that of the unpoled ones.

Dielectric response character of the 0.94NKN–0.03LS–0.03LT ceramics cannot be fitted by the Curie–Weiss law, but can be fitted by a quadratic law, $1/\varepsilon = 1/\varepsilon_{max} + (T - T_{max})^n/C'$, where n is a diffuseness index and C' is a constant, in the measured temperature range above T_m [18,19]. Fig. 4 shows the character of the dielectric response of the unpoled and poled 0.94NKN–0.03LS–0.03LT ceramics measured at 1 kHz. Using the quadratic law and the 1 kHz data to delineate the dielectric behavior above T_m of the unpoled and

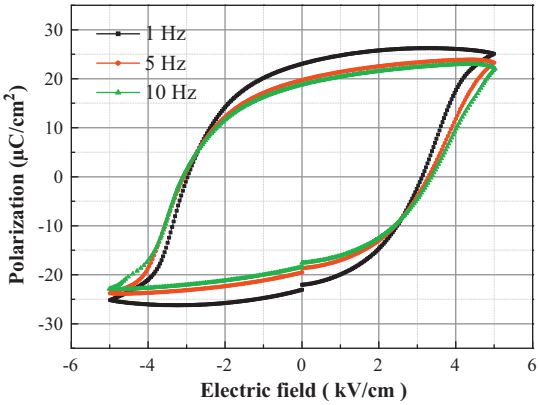

Fig. 5. Room-temperature *P–E* hysteresis loops of the 0.94NKN–0.03LS–0.03LT ceramics measured at 36.76 kV/cm and at several frequencies.

poled 0.94NKN–0.03LS–0.03LT ceramics, the diffuseness index and the constant are $n = 1.295$ and $C' = 7.727 \times 10^5$, and $n = 1.156$ and $C' = 5.882 \times 10^5$, respectively. Although 0.94NKN–0.03LS–0.03LT exhibits slight character of diffused ferroelectric phase transition, the 0.94NKN–0.03LS–0.03LT ceramics approach more closely to normal ferroelectrics since n approaches 1 for both the unpoled and poled ceramics.

3.3. Ferroelectric and piezoelectric properties

Fig. 5 shows *P–E* hysteresis loops of the 0.94NKN–0.03LS–0.03LT ceramics measured at various frequencies. Electric field strength and frequency exert great influences on the shape of the ferroelectric hysteresis loops. For the NKN-based ceramics, low frequency is favorable for different polarization mechanisms to follow up the change of the external electric field, and high electric field strength can afford enough energy for ferroelectric domains to switch and align along the direction of the external applied electric field, therefore, rather fully developed, symmetric and saturated hysteresis loops can be obtained. Due to the low relative density of the pure NKN ceramics sintered at air pressure, the value of remanent polarization P_r of the NKN ceramics is relatively small, indicating that NKN does not exhibit excellent ferroelectric property [15]. As compared to the pure NKN ceramics, the 0.94NKN–0.03LS–0.03LT ceramics present more typical hysteresis loops. At 36.37 kV/cm the 0.94NKN–0.03LS–0.03LT ceramics exhibit well developed, symmetric and saturated hysteresis loops, where no apparent pinning-down phenomenon exists, indicating that crystal structure defects are less. The value of P_r of 0.94NKN–0.03LS–0.03LT decreases from 23.06 μC/cm² at 1 Hz to 18.43 μC/cm² at 10 Hz, which corresponds well to the phenomenon of the dielectric frequency dispersion. The origin of the relaxor behavior can be attributed to the development of a quenched random field associated with the compositional/structural disorder, which is a reflection of underlying cation ordering introduced by ionic doping. The *P–E* loops are fat and nearly "square", which is considered as correlating with the tetragonal structure and the easy rotation of the tetragonal ferroelectric domains under the external electric field along the spontaneous polarization direction.

Frequency dependence of the impedance and phase degree of the 0.94NKN–0.03LS–0.03LT ceramics is shown in Figs. 6 and 7. Perfect resonance response peaks are observed in both the radial-extension-vibration-mode and the thickness-extension-vibration-mode, which provides efficient energy conversion between electrical energy and mechanical energy. Calculated from

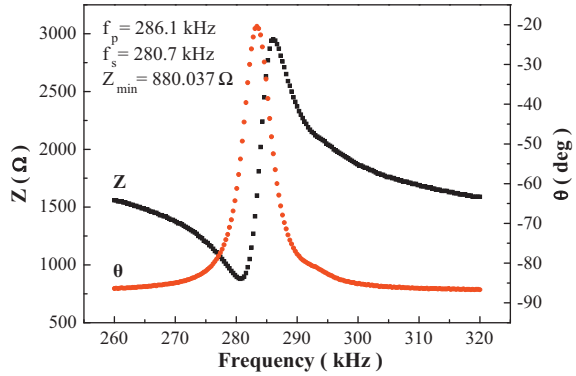

Fig. 6. Frequency dependence of impedance and phase degree of the 0.94NKN–0.03LS–0.03LT ceramic measured at low frequency.

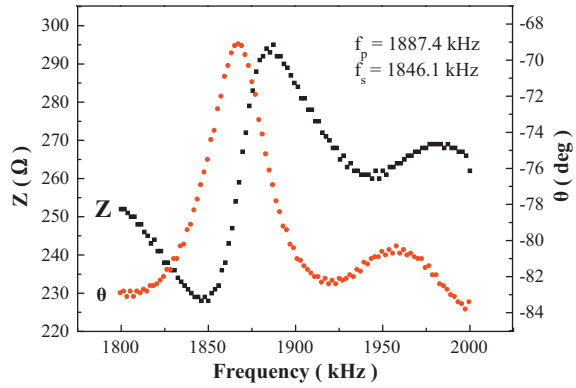

Fig. 7. Frequency dependence of impedance and phase degree of the 0.94NKN–0.03LS–0.03LT ceramic measured at high frequency.

Table 1
Electrical properties of the 0.94NKN–0.03LS–0.03LT ceramics.

P_r (μC/cm²)	E_c (kV/cm)	d_{33} (pC/N)	K_p	K_t	Q_m
23.06	3.37	228	0.220	0.230	32.19

the equations

$$K_p \approx \sqrt{\frac{f_p - f_s}{f_s} \times 2.51}, \qquad K_t^2 = \frac{\pi}{2}\frac{f_s}{f_p}\left[\tan\left(\frac{\pi}{2}\frac{f_p - f_s}{f_p}\right)\right], \quad \text{and}$$

$$Q_m = \frac{f_p^2}{2\pi \cdot f_s \cdot C^T \cdot R(f_p^2 - f_s^2)}$$

the electromechanical coupling factors K_p and K_t, and the mechanical equality factor Q_m are 0.220, 0.230 and 32.19, respectively (Table 1).

Piezoelectric property of the 0.94NKN–0.03LS–0.03LT ceramics is also shown in Table 1. As compared to the pure NKN ceramics prepared by the same conventional ceramic processing, the 0.94NKN–0.03LS–0.03LT ceramics exhibit large value of piezoelectric constant d_{33}, being 228 pC/N. Such excellent piezoelectric property can be attributed to the densification effect of the co-addition of LS–LT, where the relative density of the 0.94NKN–0.03LS–0.03LT ceramics reaches 94.73% prepared by the conventional solid-state reaction method sintered at air pressure.

4. Conclusions

0.94NKN–0.03LS–0.03LT lead-free piezoelectric ceramics with dense microstructure and good temperature stability were prepared by the conventional ceramics processing sintered

in atmosphere. XRD measurement revealed that the sintered NKN-based ceramics exhibit pure tetragonal perovskite structure induced by the co-doping of $LiSbO_3$–$LiTaO_3$. The sintered 0.94NKN–0.03LS–0.03LT ceramics exhibit excellent integral electrical properties, in which T_m is 384.7 °C and ε_m is 5351 at 0.5 kHz, the value of d_{33} is 228 pC/N, K_p is 0.220, K_t is 0.230, Q_m is 32.19, and P_r is 23.06 μC/cm^2. Such excellent electrical properties indicate that 0.94NKN–0.03LS–0.03LT are promising lead-free piezoelectric ceramics.

Acknowledgments

The authors thank the International Scientific Cooperation Project of Changzhou Scientific Bureau (Grant No. CZ2008014) and the Natural Science Fundamental Research Project of Jiangsu Colleges and Universities (Grant No. 08KJB430001) for financial support.

References

[1] J.G. Fisher, A. Bencan, J. Bernard, J. Holc, M. Kosec, S. Vernay, D. Rytz, J. Eur. Ceram. Soc. 27 (2007) 4103–4106.
[2] B. Malic, J. Bernard, J. Holc, D. Jenko, M. Kosec, J. Eur. Ceram. Soc. 25 (2005) 2707–2711.
[3] R.-C. Chang, S.-Y. Chu, Y.-F. Lin, C.-S. Hong, P.-C. Kao, C.-H. Lu, Sens. Actuators A 138 (2007) 355–360.
[4] Y. Guo, K. Kakimoto, H. Ohsato, Solid State Commun. 129 (2004) 279–284.
[5] Y. Guo, K. Kakimoto, H. Ohsato, Mater. Lett. 59 (2005) 241–244.
[6] S.W.K. Muraoka, H. Kakemoto, T. Tsurumi, H. Kumagai, Mater. Sci. Eng. B 25 (2005) 186–189.
[7] M.-R. Yang, C.-S. Hong, C.-C. Tsai, S.-Y. Chu, J. Alloys Compd. 488 (2009) 169–173.
[8] H. Du, Z. Li, F. Tang, S. Qu, Z. Pei, W. Zhou, Mater. Sci. Eng. B 131 (2006) 83–87.
[9] Z. Chen, J. Hu, Trans. Nonferr. Met. Soc. China 18 (2008) 623–626.
[10] H. Du, F. Tang, D. Liu, D. Zhu, W. Zhou, S. Qu, Mater. Sci. Eng. B 136 (2007) 165–169.
[11] M. Jiang, X. Liu, G. Chen, C. Zhou, Mater. Lett. 63 (2009) 1262–1265.
[12] M.-S. Kim, D.-S. Lee, E.-C. Park, S.-J. Jeong, J.-S. Song, J. Eur. Ceram. Soc. 27 (2007) 4121–4124.
[13] Y. Guo, K. Kakimoto, H. Ohsato, Appl. Phys. Lett. 85 (2004) 4121–4123.
[14] J. Li, Q. Sun, Solid State Commun. 149 (2009) 581–584.
[15] B. Fang, N. Jiang, R. Zhang, J. Chin. Ceram. Soc. 38 (2010) 374–380 (in Chinese).
[16] L. Wu, D. Xiao, J. Wu, Y. Sun, D. Lin, J. Zhu, P. Yu, Y. Zhuang, Q. Wei, J. Eur. Ceram. Soc. 28 (2008) 2963–2968.
[17] S.J. Zhang, R. Xia, C.A. Randall, T.R. Shrout, R.R. Duan, R.F. Speyer, J. Mater. Res. 20 (2005) 2067–2071.
[18] B. Fang, S. Pan, Q. Du, X. Zhao, H. Xu, H. Luo, J. Phys. Soc. Jpn. 79 (2010), 104703/1–6.
[19] K. Uchino, S. Nomura, Ferroelectr. Lett. 44 (1982) 55–61.